PERFORMANCES OF WOODEN LADDER-TYPE FRAMES FOR SEISMIC REINFORCEMET OF TRADITIONAL TIMBER STUCTURES

H. Tanahashi[1], M. Okamura[2] and Y. Suzuki[3]

[1]*Director, Tanahashi Structural Safety Design Institute, Sakai, Japan*
[2]*Engineer, Okamura Architecture Office, Niigata, Japan*
[3]*Professor, Ritsumeikan University, Kusatsu, Japan*
E-mail:Tana@courante.plala.or.jp

ABSTRACT :

There are many traditional timber structures, such as temples, shrines and town houses in Japan. Their rational seismic evaluation is the most important in order to mitigate probable damages caused by great earthquakes in the near future. Thus, the establishing the evaluation method and seismic reinforcement are urgently needed. We, therefore, propose wooden ladder-type frames for seismic reinforcement of traditional timber structures. In order to evaluate the proposed frame, we established the formulation of seismic performances using Pasternak model. We applied the Pasternak model to the elasto-plastic embedment behavior of wood joints, considering the orthotropic properties and the strain hardening. In order to confirm their performances, full scale experiments were carried out and the results are discussed.

KEYWORDS: traditional timber structure, Pasternak model, joint, densification, restoring force characteristics, seismic reinforcement

1. INTRODUCTION

There are many traditional timber structures, such as temples, shrines and town houses in Japan. Their rational seismic evaluation is the most important in order to mitigate probable damages caused by great earthquakes in the near future. However, the evaluation method has not been established so far because their structural systems are much different from modern structures. Also, their seismic resistances are supposed to be insufficient in many cases. Therefore, establishing the evaluation method and seismic reinforcement are urgently needed. The reinforcement for traditional timber structures should be suitable for their seismic characteristics.

The major structural elements of traditional timber structures are moment resisting frames with semi-rigid joints, mud walls and column rocking restoring forces of thick columns. The structural mechanism of semi-rigid joints is rotational embedment and friction at the contact surfaces inside the joint.

In such situations of traditional timber structures, we propose wooden ladder-type frames for seismic reinforcement. The ladder-type frame, a kind of vierendeel truss system, consists of two horizontal chords and vertical struts penetrating to the horizontal chords at the joints. Their joints are semi-rigid due to the embedment of contact interfaces inside the joints.

In order to evaluate the proposed frame, we established the formulation of seismic performances using Pasternak model (abbreviated to PM). The PM, which mechanically consists of a shear layer on the Winkler model and originated from Pasternak [1954], is an improved and refined model of a continuum compared with the conventional Winkler model. It can express the surface displacement distributions and strain profiles in the vertical direction subjected to partially compressive loads adequately. We, therefore, applied the PM to the elasto-plastic embedment behavior of wood joints, considering the orthotropic properties and the strain hardening.

The densification, or strain hardening more than 50% strains, takes place in the local area beneath the contact surfaces of the joints perpendicular to the grain, and expands to the bottom gradually as the load increases. As a result, the joints show very high ductility.

Based on such facts, the elasto-plastic embedment behavior is formulated introducing the stiffness functions which consist of two factors; the increasing factor which means the ratio of the stiffness to that of the net contact surface and the decreasing factor governed by elasto-plastic characteristics.
The full scale experiments of the proposed ladder-type frames were carried out and the results are compared with the proposed formulation and discussed.

2. ELASTO-PLASTIC EMBEDMENT MECHANISM OF WOOD

2.1 Pasternak model for the orthotropic wood

The authors applied the PM for the embedment behavior of orthotropic wood and proposed the formulation for equally loaded embedment [Tanahashi et al., 2006b] and rotational embedment of column-*Nuki* joints [Tanahashi et al., 2006a]. The important points are summarized as follows.

1. The embedded surface displacements of an orthotropic wood beam with a finite length on the rigid base due to equally distributed load on the rigid plate are expressed in Eqn. 2.1, as a representative case of the LR plane shown in Figure 1. They are expressed in a similar way in the LT plane or LTR plane which rotates from the LR plane to the LT plane by 45 degrees in Figures 2 and 3.

$$\left.\begin{aligned} W_1 &= \frac{S}{\zeta_P} \quad : \quad |x| \le L \\ W_2 &= \frac{S}{\zeta_P} e^{-\gamma|x-L|} \quad : \quad L \le |x| \le L_0 \end{aligned}\right\} \tag{2.1}$$

$$S = \frac{(1-\nu_{LR}\nu_{RL})\,qH}{E_R} : \text{Fundamental compressive displacement}$$

$$\zeta_P = 1 + \frac{1-e^{-\gamma \Delta L}}{\gamma L} = 1 + \frac{1-e^{-\gamma H \delta}}{\gamma H \lambda} : \text{Increasing ratio of stiffness}$$

$$\delta = \frac{\Delta L}{H} = \frac{L_0 - L}{H} : \text{End distance ratio to the depth}$$

$$\lambda = \frac{L}{H} : \text{Loading length ratio to the depth}$$

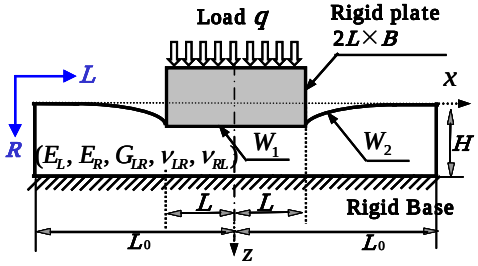

Figure 1 Orthotropic beam with a finite length on the rigid base in the LR plane

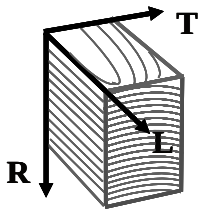

Figure 2 Three directions of wood

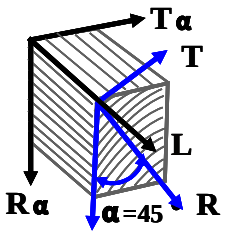

Figure 3 LTR plane

Here, ζ_P is an increasing ratio of stiffness which means the increasing ratio of the compressive stiffness in the case of $L_0 > L$ to the stiffness in the case of $L_0 = L$ where the end distance is zero. γ: characteristic value, *S*: fundamental compressive displacement when $L_0 = L$. δ is the end distance ratio and λ is the loading length ratio, respectively. The orthotropic characteristics are expressed in the fundamental compressive displacement *S* and characteristic value γ based on the elastic properties (e.g., Young's modulus E_R, shear modulus G_{LR}, Poisson's ratio ν_{LR}, ν_{RL} in the LR Plane) of the each plane. The non-dimensional characteristic value γH is decided by comparing it with finite element analyses. For

yellow cider, we proposed $\gamma H = 3$ for LR, 2.7 for LT, 2.3 for LTR and 9 for RT [Tanahashi et al., 2006b].

2. The displacement profile of a wood beam due to partial compression is assumed in a shape function $\phi(z)$ in Eqn. 2.2, which is based on the Vlasov's assumption [Vlasov et al., 1960]. The strain profile is shown in Eqn. 2.3, which is the first order differentiation of $\phi(z)$ by z. These profiles are illustrated in Figures 4 and 5. Here, η is the parameter which determines the distribution profiles. When η is zero, the displacement profile is a straight line and the strain profile is constant in the case of full compression. In the case of partial compression, $\eta > 0$ and the average strain ε_1 is reduced by the increasing ratio of stiffness from the strain ε_0 in full compression, that is, $\varepsilon_1 = \varepsilon_0 / \zeta_P$, and the strains distribute from the top ε_{1t} to the bottom ε_{1b} in Figure 5.

$$W_1\phi_1(z) = W_1 \frac{\sinh\eta(1-z/H)}{\sinh\eta} \tag{2.2}$$

$$W_1\phi_1'(z) = \frac{\partial W_1\phi_1(z)}{\partial z} = W_1 \frac{\eta\cosh\eta(1-z/H)}{H\sinh\eta} = \varepsilon_1 \frac{\eta\cosh\eta(1-z/H)}{\sinh\eta} \tag{2.3}$$

$$\varepsilon_{1t} = \varepsilon_1 \frac{\eta}{\tanh\eta} = \frac{\varepsilon_0}{\zeta_P}\frac{\eta}{\tanh\eta}, \quad \varepsilon_{1b} = \varepsilon_1 \frac{\eta}{\sinh\eta} = \frac{\varepsilon_0}{\zeta_P}\frac{\eta}{\sinh\eta}$$

2.2 Elasto-plastic Pasternak model

Referring to Figures 4 and 5, as the load increases in partial compression, the portion from the top to the depth H_y yields and the strain increases and settles at the distribution of strain $W_1\phi_2'$. Then, the elasto-plastic displacement distribution $W_1\phi_2$ and surface displacement W_1' are obtained by integrating the strain $W_1\phi_2'$ along *z* axis.

This mechanical model is developed from the elastic PM, and denotes "Elasto-plastic Pasternak model" (abbreviated to EPM). If we calculate the strain profile $W_1\phi_2'$ from the stress-strain diagram **a** of large embedment tests in Figure 6, we can simulate the elasto-plastic restoring force characteristics of partial compression in large strains.

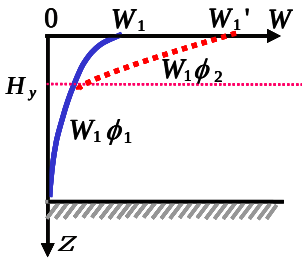

Figure 4 Displacement profile

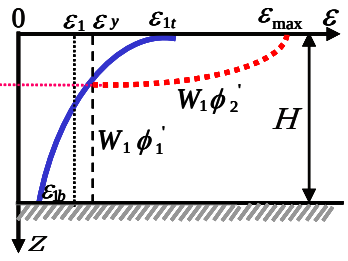

Figure 5 Strain profile

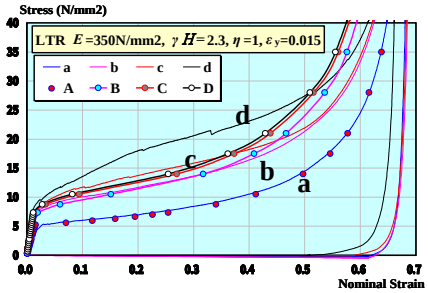

Figure 6 Stress-strain diagram of large strain embedment tests

2.3. Yielding mechanism of elasto-plastic embedment behavior

First, the stress-strain line **O-P-Q** of full compression is drawn in Figure 7, where the stress-strain diagram is combined with the strain profile. **P** is the yield point $({}_F\varepsilon_y, {}_F\sigma_y)$ of full compression. Next, the stress-strain line **O-R-S** of partial compression is drawn. **R** is the yield point $({}_P\varepsilon_y, {}_P\sigma_y)$ of partial compression. The relations in Eqn. 2.4 exist between these values.

$$\left.\begin{aligned} {}_F\sigma_y &= {}_F\varepsilon_y E \quad : \text{full compression} \\ {}_P\sigma_y &= {}_P\varepsilon_y E\zeta_P : \text{partial compression} \end{aligned}\right\} \tag{2.4}$$

Then, we assume the strain of the top becomes ${}_F\varepsilon_y$ and start to yield when the average strain reaches ${}_P\varepsilon_y$. This follows Eqn. 2.5 from the relation of Eqn. 2.3. The parameter η will be decided by the simulations.

$$ {}_P\varepsilon_y = {}_F\varepsilon_y \frac{\tanh\eta}{\eta} \qquad (2.5) $$

Here, H_y is obtained by setting Eqn. 2.3 equal to the yield strain ${}_F\varepsilon_y$ in full compression and the yielding depth ratio h_y becomes as follows.

$$ h_y = \frac{H_y}{H} = 1 - \frac{1}{\eta}\cosh^{-1}\left(\frac{{}_F\varepsilon_y}{\varepsilon_1\eta}\sinh\eta\right) \qquad (2.6) $$

Thus, the elasto-plastic displacement W_1' is shown as,

$$ W_1' = \int_0^H W_1\phi_1'\,dz + \int_0^{H_y}[W_1\phi_2' - W_1\phi_1']\,dz \qquad (2.7) $$

The stress-strain relation of fully compressive displacements in large stain levels more than ε_y in the radial direction (LR plane) was formulated by Norimoto [1993].

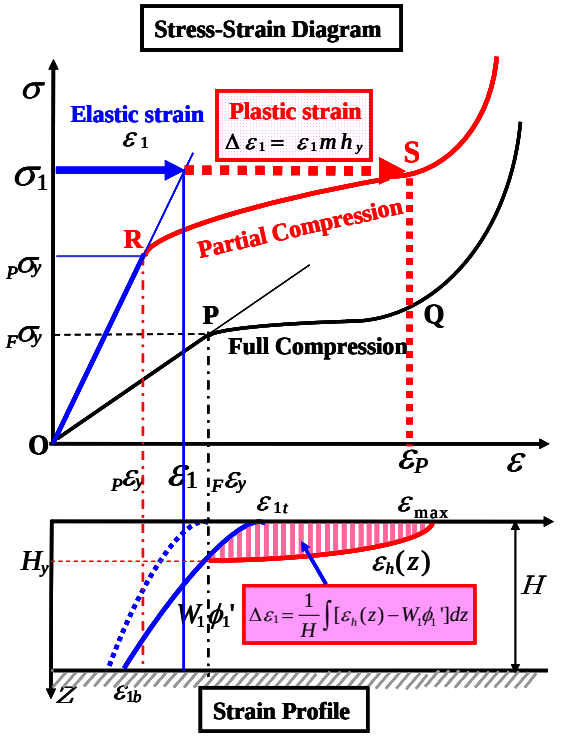

Figure 7 Yielding mechanism of partial compression

Then, we set $\varepsilon_h(\sigma)$ equal to $\varepsilon_h(z)$ which corresponds to $W_1\phi_2'$, and the increased plastic strain $\Delta\varepsilon_1$ is expressed in Eqn. 2.8 by mh_y times of the elastic strain ε_1 as shown in Figure 7 conceptually. Here, *m* denotes the equivalent multiplying factor to the elastic strain.

$$ \Delta\varepsilon_1 = \frac{1}{H}\int_0^{H_y}[W_1\phi_2' - W_1\phi_1']\,dz = \frac{1}{H}\int_0^{H_y}[\varepsilon_h(z) - W_1\phi_1']\,dz = \frac{\varepsilon_1 m H_y}{H} = \varepsilon_1 m h_y \qquad (2.8) $$

Thus, the increased elasto-plastic strain ε_P is obtained as follows.

$$ \varepsilon_P = \frac{W_1'}{H} = \frac{1}{H}\int_0^H W_1\phi_1'\,dz + \frac{1}{H}\int_0^{H_y}[W_1\phi_2' - W_1\phi_1']\,dz = \varepsilon_1 + \varepsilon_1 m h_y = \varepsilon_1(1 + m h_y) \qquad (2.9) $$

Simulated curves **A**, **B**, **C** and **D** of embedment behaviors in large strains are shown in Figure 6 based on Norimoto's formulation. The simulations are in good agreement with the test results in small strain levels except for **D**. However, these simulations are not so simple and rather complex. Thus, we propose simple forms of the yielding depth ratio h_y and the equivalent multiplying factor m for practices in Eqn. 2.10. κ denotes the yielding ratio of the working stress to the yield stress. The yielding depth ratio $h_y = 0$ if $\kappa < 1$, and $h_y = 1$ if obtained h_y is larger than 1. Under this condition, the relation Eqn. 2.5 is replaced by Eqn. 2.11.

$$ h_y = \frac{1}{\eta}\ln\left(\frac{\varepsilon_1\eta}{{}_F\varepsilon_y}\right) = \frac{1}{\eta}\ln\kappa, $$

$$ m = C\left(1 - \frac{{}_F\varepsilon_y}{\varepsilon_1\eta}\right) = C\left(1 - \frac{1}{\kappa}\right) \qquad (2.10) $$

where, $0 \le h_y \le 1$, C : constant, $\kappa = \dfrac{\varepsilon_1\eta}{{}_F\varepsilon_y} = \dfrac{\varepsilon_1}{{}_P\varepsilon_y}$: yielding ratio.

$$ {}_P\varepsilon_y = \frac{{}_F\varepsilon_y}{\eta} \qquad (2.11) $$

3. SIMPLE FORMULATION WITH STIFFNESS FUNCTIONS

3.1 Stiffness function for rotational embedment

We assume the following conditions for the formulation of the rotational embedment and illustrate the mechanism of T-type joint with the depth *H* and the width *B* of the strut, and the depth 2*L* of the chord in Figure 8.

1. The chord is perfectly rigid and only the strut embeds rotating perpendicular to the grain subjected to the moment *M*.
2. The contact length *L* between the strut and the chord is constant for T type joint.
3. The reactions of the strut due to rotational embedment take place according to the contact length L based on EPM both inside and outside the contact surface.
4. The vertical reaction $F = \mu R$ is proportional to the reaction *R* perpendicular to the grain as Coulomb friction.

$$\theta_P = \frac{M}{\sum K_{R0}\zeta_R(\theta) + \sum \mu K_{F0}\zeta_F(\theta)} \tag{3.1}$$

$$\left.\begin{aligned} \zeta_R(\theta) &= \frac{1 + \frac{3}{\gamma L}[(1+\frac{1}{\gamma L})(1-e^{-\gamma\Delta L}) - \frac{\Delta L}{L}e^{-\gamma\Delta L}]}{1+mh_y} : \text{stiffness function of rotation} \\ \zeta_F(\theta) &= \frac{1 + \frac{2}{\gamma L}(1-e^{-\gamma\Delta L})}{1+mh_y} : \text{stiffness function of friction} \end{aligned}\right\} \tag{3.2}$$

$K_{R0} = \frac{2EBL^3}{3H}$: rotational stiffness of the net contact area

$K_{F0} = \frac{EBL^2}{2}$: frictional stiffness of the net contact area

μ : coefficient of friction,

Practical formula : $m = C(1-1/\kappa)$, $h_y = \frac{H_y}{H} = \frac{1}{\eta}\ln\kappa : (0 \le h_y \le 1)$ (3.3)

where, $\kappa = \frac{\theta\eta}{\theta_y} = \frac{\varepsilon\eta}{{}_F\varepsilon_y}$: yielding ratio

The moment *M*-rotation angle θ_P relation is expressed using the stiffness functions for a chord-strut joint in Eqn. 3.1. It is noted that θ_P is the increased elasto-plastic rotation angle in the case of the elastic rotation angle θ and the corresponding elastic moment *M*. The symbol $\sum$ means the summation of stiffness functions and stiffness of embedment reactions of R_1 and R_2 in Figure 8.

The numerators in Eqn. 3.2 are the increasing factors which express the increasing ratio of rotational or frictional stiffness to those of the net contact area of the chord-strut joint. The denominators in Eqn. 3.2 are the strain softening or hardening factors governed by yielding or densification in the plastic state. h_y and m are the parameters in Eqn. 3.3 if the strain in Eqn 2.10 is replaced by the rotation angle. They are expressed by κ which is the yielding ratio of the working rotation angle to the yield rotation angle θ_y. Here, θ_y is equal to ${}_F\varepsilon_y L$, i.e., the yielding rotation angle when the maximum strain beneath the edge reaches ${}_F\varepsilon_y$.

4. EXPERIMENTS AND SIMULATION

4.1 Experiment of T-type joint

The experimental setup of T-type joint is shown in Figure 9. It is composed of a strut of *hinoki* cypress crossed by wood blocks of *hinoki* cypress. The specimens of LT planes were tested. The strut surface inside the joint was subjected to rotational compression shown in Figure 8.

The joint was subjected to one-way horizontal forces at the top of the strut. Each specimen was loaded with Teflon (*polytetrafluoroethylene*) sheets (thickness 0.8mm) and without them between the contact interface of chord-strut joints in order to measure the frictional and horizontal reaction separately. The friction is decreased by the Teflon sheet, but the coefficient of friction $\mu = 0.1$ remains, which is based on the maker's data. However, it has not been confirmed yet experimentally. Therefore, we carried out friction experiments in order to confirm the friction effects under the embedded conditions. The coefficients of friction resulted in around 0.5 without Teflon sheet and 0.1 with it.

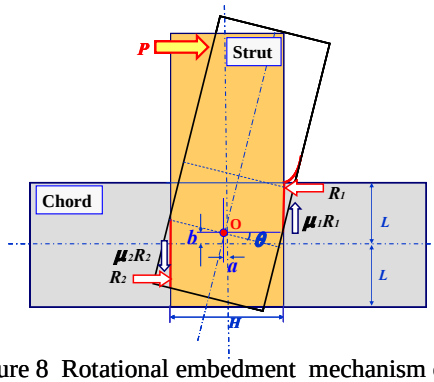

Figure 8 Rotational embedment mechanism of T-type joint

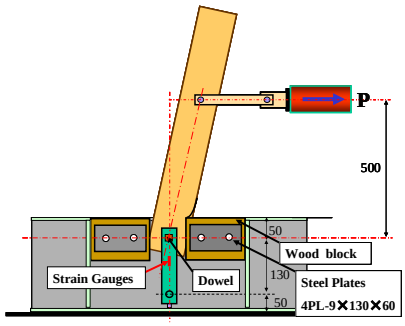

Figure 9 Experimental setup of T-type joint

4.2 Experiment of ladder-type frames

The experimental setup and the analytical model of a ladder-type frame between two vertical columns are shown in Figure 10 and 11. The static multi-cycle horizontal forces are loaded at the top of the column.

The test specimens are two types; one is for temples or shrines, and the other is for townhouses. Horizontal displacements of column top and strains of struts and chords, rotations of joints were measured.

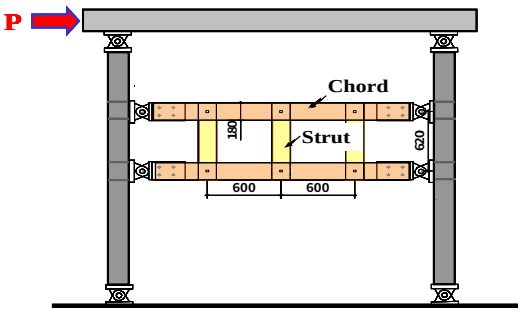

Figure 10 Experimental Setup of ladder–type frame with columns

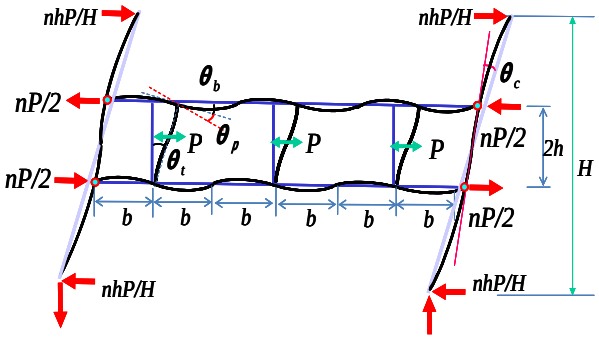

Figure 11 Analytical model of ladder–type frame with columns

4.3 Moment–rotation angle relation of ladder-type frames

The rotation consists of four kinds of rotations in Eqns 4.2-4.4 and the moment-rotation angle relations of ladder-type frames with two columns are formulated in Eqn 4.1 when the ladder-type frame is set at the middle of the floor height. Here, I_bE_b, I_tE_t and I_cE_c are bending stiffness of the beam, strut and column, respectively. *n* is the number of the struts. If their bending stiffness are large enough, the rotation angles except the rotation due to the embedment are negligible.

$$\theta = \theta_P + \theta_b + \theta_t + \theta_c \tag{4.1}$$

$$\theta_P = \frac{M}{\sum K_{R0}\zeta_R(\theta) + \sum \mu K_{F0}\zeta_F(\theta)} : \text{rotation due to embedment} \tag{4.2}$$

$$\theta_b = \frac{Mb}{6E_bI_b} : \text{rotation due to bending of the beam} \tag{4.3}$$

$$\theta_t = \frac{Mh}{3E_tI_t} : \text{rotation due to bending of the strut} \tag{4.4}$$

$$\theta_c = \frac{nMH}{12E_cI_c}\left(1-\frac{2h}{H}\right)^2 : \text{rotaion due to bending of the column} \tag{4.5}$$

4.4 Experimental results and discussion

The moment-rotation angle relations of the experiments are shown with simulated results in typical cases in Figure 12 for shrines and temples and in Figure 13 for townhouses.
The simulations based on EPM are in good agreement with the experimental results, although the parameters might be revised. It is noted that the resisting moments increase up to large displacements more than 0.15 radian after yielding. Such ductile performances are mainly due to the densification of wood. The seismic reinforcement by ladder-type frames is shown to be very effective for large displacements.

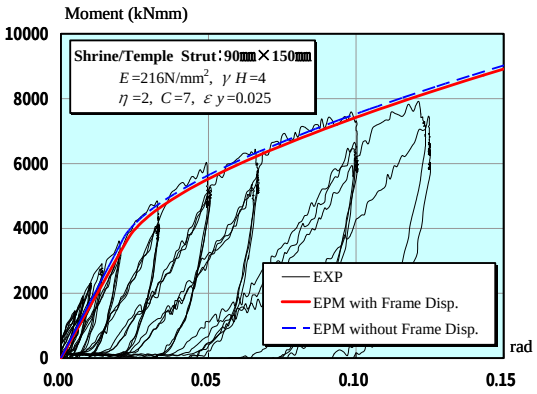

Figue 12 Test result and EPM Simulation for Shrines and Temples

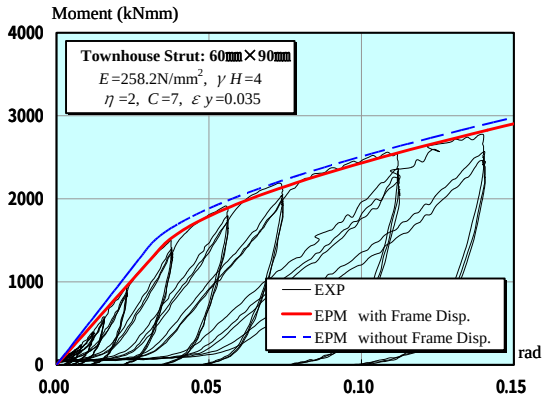

Figure 13 Test result and EPM Simulation for Townhouses

5. CONCLUSIONS

The major conclusions of this study are summarized as follows.

1. The elasto-plastic embedment mechanism of orthotropic wood is analyzed considering the densification based on the elasto-plastic Pasternak model.

2. The elasto-plastic embedment behaviors are formulated in simple forms using the stiffness functions for rotational embedment of traditional joints.
3. The wooden ladder-type frames are proposed for seismic reinforcement for traditional timber structures, and the full scale experiments of the proposed frames were carried out for their experimental verification.
4. The simulations based on the elasto-plastic Pasternak model are discussed with the experimental results, and are shown to be in good agreement with the results if the parameters are assumed appropriately.
5. The proposed wooden ladder-type frames are very ductile, mainly due to the densification of wood, and their seismic reinforcement is shown to be very effective for large displacements.

ACKNOWLEDGEMENT

The part of this research was carried out as a cooperative research of Wood Composite Hall, Research Institute for Sustainable Humanosphere, Kyoto University, and also supported by the Grant-in-Aid for Scientific Research (S) (No.19106010, Principal Researcher: Yoshiyuki Suzuki) of Japan Society for the Promotion of Science.

REFERENCES

Pasternak P.L.(1954), On a new method of analysis of an elastic foundation by means of two foundation constants, *Gosudarstvennoe Izdatelstvo Literaturi po Stroitelstuve i Arkhitekture*, Moscow, (in Russian).

Vlasov V.Z., and Leont'ev N.N.(1966), Beams, plates and shells on elastic foundations, Israel Program for Scientific Translations, Jerusalem, (Original Russian version 1960).

Norimoto M.(1993), Large compressive deformation in wood, *Mokuzai Gakkaishi*, **39**,:**8**, 867-874 (in Japanese).

Tanahashi H., Shimizu H., and Suzuki Y.(2006a), Formulation of elasto-plastic moment-resisting performance of timber connections using Pasternak model, Proc. WCTE2006, Portland, Oregon, USA.

Tanahashi H., Shimizu H., and Suzuki Y.(2006b), Elastic surface displacements of orthotropic wood due to partial compression based on Pasternak model, *J. Struct. Constr. Eng*., AIJ, **609,129-136** (in Japanese).

Tanahashi H., Shimizu H., Horie H., Yang P., and Suzuki Y.(2008), Elastic embedded displacements of orthotropic wood with a finite length based on Pasternak model, *J. Struct. Constr. Eng*., AIJ, **73, 625,** 417-424 (in Japanese).

Tanahashi H., Okamura M., and Suzuki Y.(2008), Simple formulation of elasto-plastic embedment behaviour of orthotropic wood considering densification, Proc. WCTE2008, Miyazaki, Japan.